Acta Crystallographica Section B
Structural Science, Crystal Engineering and Materials
ISSN 2052-5192

$C_6H_4S_2AsCl$: description and interpretation of an incommensurately modulated molecular crystal structure

Ronald C. Bakus II,[a] David A. Atwood,[a] Sean Parkin,[a] Carolyn P. Brock[a]* and Vaclav Petricek[b]

[a]Department of Chemistry, University of Kentucky, Lexington, KY 40506-0055, USA, and [b]Institute of Physics of the Academy of Sciences of the Czech Republic, v.v.i., Na Slovance 2, Praha 8, 182 21, Czech Republic

Correspondence e-mail: cpbrock@uky.edu

Received 15 November 2012
Accepted 28 June 2013

B-IncStrDB Reference:
8082ERT5uS

Crystals of 2-chloro-benzo-1,3,2-dithiarsole have a strongly modulated structure that can be solved and refined with relative ease in a $P\overline{1}$, $Z' = 17$ approximate supercell but that is better described as incommensurate. Two conventional refinements (different superstructure approximations that differ in the placement of their crystallographic inversion centers) and a (3 + 1)-dimensional superspace refinement are all nearly equally successful, at least as measured by the usual agreement factors; the data integration, however, shows that the incommensurate description is preferable. The overall packing is determined by the stacking of the aromatic rings and probably by the segregation of As and Cl atoms to give short As···Cl contacts. A refinement of the average ($Z' = 1$) structure shows that there are two basic orientations of the C_6S_2 plane, but that those orientations must be correlated in several directions to avoid impossibly short intermolecular contacts. Along the modulation vector **q** the orientation of the C_6S_2 plane varies smoothly, but **q** is not a direction in which the molecules are in contact. Along the directions in which the molecules are in contact the orientation of the C_6S_2 plane alternates; there are also positional shifts. The single modulation **q** relieves packing problems in several different directions well enough that crystals that diffract well can be grown.

1. Introduction

The compound 2-chloro-benzo-1,3,2-dithiarsole (hereafter, DTAsCl) was synthesized as part of a study of reactions of dithiols with As and Sb (Shaikh, Bakus *et al.*, 2006; Shaikh, Parkin *et al.*, 2006). Unlike the Sb analog, which has a 'normal' (*Pbca*; $Z' = 1$) structure, DTAsCl appears to crystallize with a very large, triclinic cell. While we initially described the structure in space group $P\overline{1}$ with $Z' = 17$, we later realized the structure is modulated incommensurately. Once a structural model had been refined the challenge was to understand why the structure was so unusually complex.

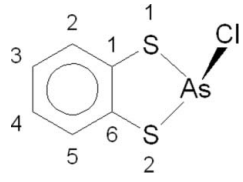

A search of the Cambridge Structural Database (hereafter, the CSD; Allen, 2002, Version 5.33 plus updates through August 2012) for closely related compounds (*i.e.* group 15 atom and halogen atom variable; other substituents allowed on the S_2C_6 ring) turned up only two: QENTAF, the Sb

Table 1
Experimental details for the refinements in the commensurate approximation.

For all structures: $C_6H_4AsClS_2$, M_r = 250.58, triclinic, $P\overline{1}$, Z = 34. Experiments were carried out at 90 K with Mo $K\alpha$ radiation using a Nonius KappaCCD diffractometer. Absorption was corrected for by multi-scan methods, *SCALEPACK* (Otwinowski & Minor, 2006). Refinement was on 859 parameters with 3978 restraints. H-atom parameters were constrained.

	Approximation (I)	Approximation (II)
Crystal data		
a, b, c (Å)	12.3533 (2), 22.3789 (3), 26.6255 (5)	
α, β, γ (°)	76.7415 (7), 80.0542 (8), 76.8076 (7)	
V (Å^3)	6918.9 (2)	
μ (mm^{-1})	4.93	
Crystal size (mm)	0.18 × 0.12 × 0.10	
Data collection		
T_{min}, T_{max}	0.47, 0.64	
No. of measured, independent and observed [$I > 2\sigma(I)$] reflections	48 421, 24 396, 8774	
R_{int}	0.052	
Refinement		
$R[F^2 > 2\sigma(F^2)]$, $wR(F^2)$, S	0.042, 0.107, 1.06	0.041, 0.105, 1.04
No. of reflections	24 396	
No. of parameters	859	
No. of restraints	3978	
H-atom treatment	H-atom parameters constrained	
$\Delta\rho_{max}$, $\Delta\rho_{min}$ (e Å^{-3})	1.74, −1.57	1.40, −1.59

Computer programs: *COLLECT*, *DENZO-SMN* (Nonius, 1997), *SHELXS*97 (Sheldrick, 2008*a*), *SHELX*97, *SHELXL*97 (Sheldrick, 2008*a*), *Mercury* (Macrae *et al.*, 2008) and local procedures.

structure mentioned above, and DAXLOD (Kisenyi *et al.*, 1985), which differs from DTAsCl in having the H atom on atom C3 replaced by a methyl substituent. DAXLOD is also an unremarkable structure ($P2_1/c$; Z' = 1). Another related structure is VEMKED (Becker *et al.*, 1990; $P2_1/n$, Z' = 1), which is like the Sb compound except for the substitution of one of the S atoms by an O atom.

In addition to wanting to understand why the DTAsCl structure is modulated in such an unusual way we wanted to compare the two approaches to structure refinement, *i.e.* a conventional refinement (Sheldrick, 2008*a*) of the approximate, Z' = 17 superstructure and a superspace refinement (*JANA*: Petříček *et al.*, 2006) of an incommensurate description. Such a comparison was made previously by Schönleber & Chapuis (2004) for the modulated structure of quininium (*R*)-mandelate. We expected the agreement factors for the two refinements to be similar (Wagner & Schönleber, 2009), but wanted to know whether the incommensurate description would provide structural insights that would have been missed had we not gone beyond the commensurate approximation. A surprising result of doing the refinement in two different ways was finding two superstructure approximations that fit the data nearly equally well. The two models are very similar except for having their crystallographic inversion centers located in quite different environments.

2. Experimental

2.1. Synthesis

The compound was prepared and the crystals were grown by the methods outlined by Shaikh, Bakus *et al.* (2006) for several other cyclized halo-arsenic dithiolates.

2.2. First conventional structure determination [commensurate superstructure approximation (I)]

Data were collected in 2004 after flash cooling a crystal to 90 K (Nonius KappaCCD diffractometer equipped with a CRYOCOOL-LN2 low-temperature system from CRYO Industries of America, Manchester, NH; Mo $K\alpha$ radiation from a fine-focus sealed tube). No special procedure was followed during data collection or data processing even though the unit cell was large (Table 1). It was immediately apparent, however, that many of the reflections are very weak; of 24 396 unique reflections measured to $(\sin\theta/\lambda)_{max}$ = 0.60 Å^{-1} (25° for Mo $K\alpha$ radiation) only 8772 (36%) had $I > 2\sigma(I)$.

The structure was solved without difficulty in $P\overline{1}$ using *SHELXS* (Sheldrick, 2008*a*). While the Z' value found (17) is exceptionally high, there are only 17 × 10 non-H atoms in the asymmetric unit of which 68 have at least 16 e$^-$. Furthermore, there are only 4 × 17 = 68 independent H atoms.

Refinement with *SHELXL* (Sheldrick, 2008*a*) to $R < 0.05$ was straightforward but required the application of many restraints. The instruction *SAME* (effective e.s.d. 0.015) kept the 1,2 and 1,3 distances in the 17 independent molecules (labeled A through to Q; Fig. 1)

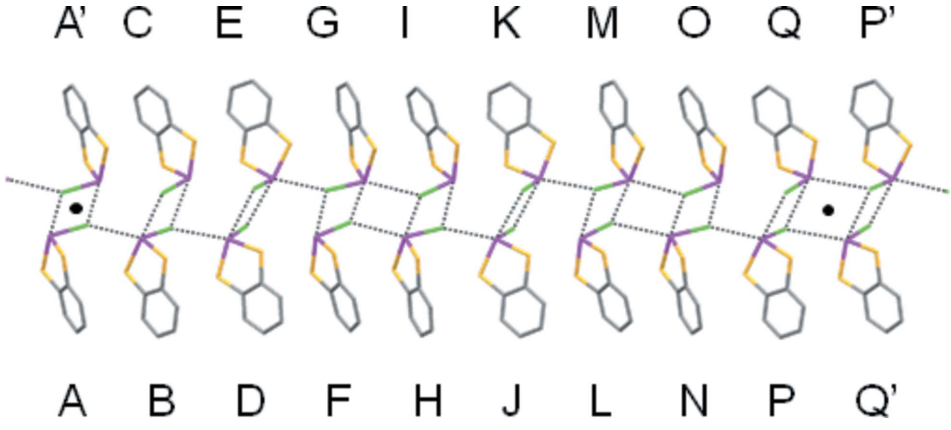

Figure 1
The unique part of the ribbon found in the structure of $C_6H_4S_2AsCl$ as originally refined in the commensurate approximation. The plane of view is approximately $(\overline{1}\ \overline{1}\ 4)_{17}$; the ribbon axis is $[1\ 3\ 1]_{17}$. As···Cl contacts shorter than the sum of the van der Waals radii (1.85 + 1.75 = 3.60 Å; Bondi, 1964) are marked.

Table 2
Distances (Å) for the three superspace refinements made with *JANA*2006.

Models (I), (II) and (III) are the commensurate $t_0 = 0$, commensurate $t_0 = 1/2$, and incommensurate refinements. Note that the variations in these distances are so small that t plots of them would be essentially straight lines. Values from the *SHELXL* refinements for models (I) and (II) are essentially the same to within their uncertainties.

Type	Model	Average	Minimum	Maximum	Range
As—Cl1	(I)	2.294 (4)	2.277 (4)	2.312 (4)	0.035
	(II)	2.294 (4)	2.273 (4)	2.313 (4)	0.040
	(III)	2.293 (4)	2.270 (4)	2.315 (4)	0.045
As—S1	(I)	2.209 (3)	2.202 (3)	2.217 (3)	0.015
	(II)	2.209 (3)	2.201 (3)	2.219 (3)	0.018
	(III)	2.209 (3)	2.200 (3)	2.221 (3)	0.021
As—S2	(I)	2.215 (3)	2.181 (3)	2.240 (3)	0.059
	(II)	2.215 (3)	2.184 (3)	2.241 (3)	0.057
	(III)	2.216 (3)	2.193 (3)	2.242 (3)	0.049
S1—C1	(I)	1.763 (11)	1.749 (11)	1.772 (11)	0.023
	(II)	1.763 (11)	1.750 (11)	1.772 (11)	0.022
	(III)	1.764 (11)	1.756 (11)	1.772 (11)	0.016
S2—C6	(I)	1.765 (10)	1.752 (10)	1.777 (10)	0.025
	(II)	1.765 (10)	1.749 (10)	1.779 (10)	0.030
	(III)	1.765 (10)	1.749 (10)	1.779 (10)	0.030
C1—C2	(I)	1.397 (14)	1.380 (14)	1.415 (14)	0.035
	(II)	1.397 (14)	1.380 (14)	1.415 (14)	0.035
	(III)	1.397 (14)	1.379 (14)	1.415 (14)	0.036
C1—C6	(I)	1.395 (16)	1.380 (15)	1.406 (15)	0.026
	(II)	1.395 (16)	1.378 (15)	1.407 (17)	0.029
	(III)	1.395 (16)	1.379 (15)	1.407 (17)	0.028
C2—C3	(I)	1.380 (16)	1.361 (16)	1.402 (16)	0.041
	(II)	1.380 (16)	1.359 (16)	1.401 (16)	0.042
	(III)	1.381 (16)	1.357 (16)	1.402 (15)	0.045
C3—C4	(I)	1.388 (16)	1.364 (17)	1.415 (17)	0.051
	(II)	1.388 (16)	1.364 (16)	1.414 (17)	0.050
	(III)	1.388 (16)	1.365 (16)	1.416 (17)	0.051
C4—C5	(I)	1.381 (14)	1.368 (14)	1.393 (14)	0.025
	(II)	1.381 (14)	1.370 (14)	1.395 (14)	0.025
	(III)	1.380 (14)	1.365 (14)	1.392 (14)	0.027
C5—C6	(I)	1.397 (15)	1.372 (15)	1.412 (15)	0.040
	(II)	1.397 (15)	1.374 (15)	1.412 (15)	0.038
	(III)	1.397 (15)	1.368 (15)	1.419 (15)	0.051

similar (distances available in the supplementary material[1] for the final *SHELXL* refinement; see also Table 2). The instruction *DELU* (effective e.s.d. 0.005) imposed a rigid-bond restraint on the 1,2 (*i.e.* bonded) and 1,3 interatomic vectors, and the instruction *ISOR* (effective e.s.d. 0.01) was applied to the C-atom ellipsoids to try to keep them roughly equi-dimensional. In spite of these restraints three of the 102 C atoms had non-positive-definite displacement ellipsoids when the refinement converged.

Table 3
Distribution of non-bonded contacts in the final $Z' = 17$ refinements of superstructure approximations (I) and (II).

The sum of the van der Waals radii is 3.60 Å for both As···Cl and S···S contacts.

Distance	As···Cl (in dimers)		As···Cl (in ribbon)		S···S	
range (Å)	(I)	(II)	(I)	(II)	(I)	(II)
3.30–3.35	4	4	–	–	–	–
3.35–3.40	4	5	–	–	2	2
3.40–3.45	5	5	2	3	2	4
3.45–3.50	2	–	5	4	4	–
3.50–3.55	1	2	2	3	–	4
3.55–3.60	1	1	2	–	2	–
3.60–3.65	–	–	–	1	2	–
3.65–3.70	–	–	1	1	3	6
3.70–3.75	–	–	1	–	2	–
3.75–3.80	–	–	–	1	–	1
3.80–3.85	–	–	1	1	–	–
3.85–3.90	–	–	1	–	–	–
3.90–3.95	–	–	–	2	–	–
3.95–4.00	–	–	2	1	–	–
Median	3.41	3.39	3.51	3.52	3.59	3.53
Average	3.41	3.41	3.62	3.62	3.55	3.55

Using the display program *Mercury* (Macrae *et al.*, 2008) we found that the 17 molecules seemed to be organized by quite short As···Cl contacts into dimers, and by somewhat longer As···Cl contacts into ribbons that run parallel to [1 3 1] of the conventional $Z' = 17$ cell (Fig. 1 and Table 3). There are also some inter-ribbon S···S contacts to atom S2 (Fig. 2) that are shorter than twice the van der Waals radius of an S atom (1.80 Å; Bondi, 1964). The repeat distance along $[1\ 3\ 1]_{17}$[2] is 81.74 Å, which corresponds to 17 dimers, of which nine are independent. One of the nine (A/A′) is located on a crystallographic inversion center; two other dimers (P/Q and Q′/P′) are related by a different inversion center.

Within the dimer ribbons there are two basic molecular orientations along with some intermediate variants. These orientations are most easily described by the angle made by the dithiolate (*i.e.* S_2C_6) plane with the plane $(\bar{1}\ \bar{1}\ 4)_{17}$ (Fig. 2). These dithiolate angles (Table 4) range from 68 to 29°, with molecules A and N at the upper end of that range and molecules J and K at the lower. These angles eventually proved to be the key to understanding the modulation.

We sorted the 17 molecules into groups based on the value of this interplanar angle and then required that the (harmonic) anisotropic displacement parameters (hereafter, ADPs) for the corresponding atoms of the S_2C_6 units within each group be equal. Molecules within each of the (three) groups are well related by pseudo-translation or pseudo-inversion so that their displacement ellipsoids are likely to be similar. The groups (Table 4) were first chosen by looking for gaps in the values of the $(S_2C_6),(\bar{1}\ \bar{1}\ 4)_{17}$ angle; initially we used four groups but then decided that using three was better. In one case [molecule (I)] the boundary was moved slightly off the gap because

[1] Supplementary data for this paper are available from the IUCr electronic archives (Reference: SN5121). Services for accessing these data are described at the back of the journal.

[2] The subscripts '17' and 'bas' are used to distinguish between the approximately commensurate $Z' = 17$ supercell and the basic cell of the incommensurate description.

Table 4
Angles (°) between the dithiolate (S_2C_6) planes and the plane $(\bar{1}\,\bar{1}\,4)_{17}$ for the final superstructure approximations sorted by value; there is no implication that the two molecules in a line correspond.

The boundaries of the groups to which *EADP* instructions were applied (see text) are shown. The estimated uncertainties are just over 0.1°.

Approximation (I)		Approximation (II)	
Molecule	Angle	Molecule	Angles
A	68.1	10	67.9
N	67.8	17	67.8
G	66.8	3	67.5
O	66.8	13	65.7
H	64.6	7	65.5
F	64.5	14	63.4
I	61.4	6	63.1
M	59.5	4	59.1
L	56.8	11	54.0
C	51.0	16	53.2
B	46.8	1	47.2
Q	43.2	9	40.6
P	36.0	8	39.3
D	35.2	2	33.1
E	30.9	15	31.5
K	28.7	12	29.4
J	28.6	5	28.1

doing so led to a significant improvement in the refinement. *DELU* (but not *ISOR*) restraints (effective e.s.d. 0.005) were applied to all atoms. No constraints were applied to the ADPs of the As and Cl atoms. We tried allowing unconstrained refinement of the ADPs for the 34 S atoms, but the resulting ellipsoids were unsatisfactory.

There were no convergence problems and the final refinement is satisfactory by standard criteria (Table 1; the ellipsoids are shown in the supplementary material). The agreement factors are low, all [3(6 + 2) + 17(2) = 58] independent displacement ellipsoids are physically reasonable, and the bond lengths (which were restrained) do not vary much (see supplementary material and Table 2).[3] There are, however, significant peaks and troughs in the final difference-Fourier map. The largest features are close to As atoms and some S atoms.

A crystal of this compound was also studied at 293 K to see whether the unit cell at room temperature might be different from that found after flash cooling to 90 K. We found no simpler cell at room temperature. Some experiments were made to see if cooling a crystal slowly might allow the structure to lock into some smaller unit cell, but we found no evidence of any such transition.

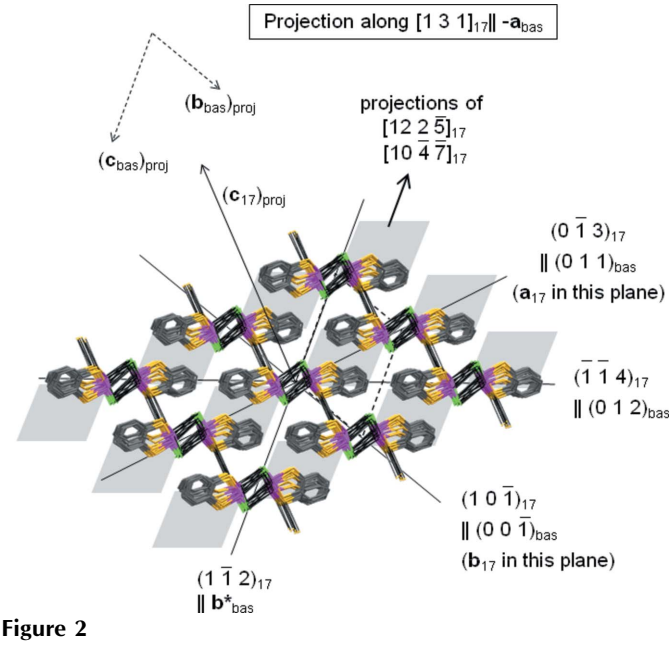

Figure 2
A view of the packing along $[1\,3\,1]_{17} \parallel -\mathbf{a}_{bas}$, *i.e.* along the axis of the ribbons shown in Fig. 1. Traces of important planes, all of which include the view direction, are marked; they are labeled both for the approximate commensurate supercell having $Z' = 17$ and for the basic cell of the incommensurate description. Also marked are the short S···S contacts. The projections of axes $\mathbf{b}_{bas}$ and $\mathbf{c}_{bas}$ appear as dashed lines. The filled parallelograms isolate the areas of the inter-ribbon contacts that are probably most important in determining the modulation. The angles between $[1\,3\,1]_{17} \parallel -\mathbf{a}_{bas}$ and $[12\,2\,\bar{5}]_{17} \parallel -\mathbf{c}^*_{bas}$ is 81.3°; the angle with $[10\,\bar{4}\,\bar{7}]_{17} \parallel [2\,0\,\bar{1}]_{bas}$ is 126.1°.

2.3. Structure description in (3 + 1)-dimensional superspace

Given the low fraction of data with $I > 2\sigma(I)$, the very high, and prime, Z' value, and the obvious modulation (Fig. 1), the possibility of an incommensurate structure had to be considered. (The degree of sparseness of the diffraction peaks can be seen in the reconstructed reciprocal-lattice slices *hk*0, *h*0*l* and 0*kl*, which are available for the basic cell with the supplementary material.) In 2009 the original frames were re-integrated by R. Hooft, then of Bruker AXS Delft, using Version 14 of the software package *EvalCCD* (Duisenberg *et al.*, 2003), which allows for incommensurate modulations. The data were integrated again in 2010 by A. M. M. Schreurs with Version 15 of the same program (Schreurs *et al.*, 2010). Two interfering crystallites (perhaps resulting from crystal cracking) were found during the second integration. The final basic cell has $Z = 2$ and dimensions:

(i) 4.8103 (2), 8.3518 (3), 11.0375 5) Å and

(ii) 70.123 (2), 81.344 (3), 79.003 (3)°.

The one-dimensional modulation vector **q** was determined to be

$$0.29482\,(12)\mathbf{a}^*_{bas} - 0.18747\,(12)\mathbf{b}^*_{bas} - 0.4715\,(2)\mathbf{c}^*_{bas} \qquad (1)$$

or

$$[5.012\,(2)/17]\mathbf{a}^*_{bas} - [3.187\,(2)/17]\mathbf{b}^*_{bas} - [8.016\,(3)/17]\mathbf{c}^*_{bas}. \qquad (2)$$

The incommensurability of the modulation is clear, especially in the $\mathbf{b}^*_{bas}$ direction.

Satellite reflections through the fourth order were considered. After integration an absorption correction was made with *SADABS* (Sheldrick, 2008*b*).

Comparison of the $P\bar{1}$ basic cell ($Z' = 1$; two partial occupancy molecular orientations; see below) and the approximate

[3] The somewhat wider range of the As—S2 distances may be related to the presence of some short intermolecular S2···S2 interactions.

Z' = 17 supercell shows that they are well related by the transformation

$$\begin{bmatrix} \mathbf{a}_{17} \\ \mathbf{b}_{17} \\ \mathbf{c}_{17} \end{bmatrix} = \begin{bmatrix} -1 & 1 & -1 \\ -4 & -1 & 0 \\ -4 & 2 & 1 \end{bmatrix} \begin{bmatrix} \mathbf{a}_{\rm bas} \\ \mathbf{b}_{\rm bas} \\ \mathbf{c}_{\rm bas} \end{bmatrix}$$

$$\begin{bmatrix} \mathbf{a}_{\rm bas} \\ \mathbf{b}_{\rm bas} \\ \mathbf{c}_{\rm bas} \end{bmatrix} = \begin{bmatrix} -1/17 & -3/17 & -1/17 \\ 4/17 & -5/17 & 4/17 \\ -12/17 & -2/17 & 5/17 \end{bmatrix} \begin{bmatrix} \mathbf{a}_{17} \\ \mathbf{b}_{17} \\ \mathbf{c}_{17} \end{bmatrix}. \quad (3)$$

The ribbons shown in Fig. 1 run along the $\mathbf{a}_{\rm bas}$ axis (Fig. 2). When the modulation vector $\mathbf{q}$ is transformed from the basic cell to the Z' = 17 supercell it has the components

$$(-0.0108, -1 + 0.0084, -2 - 0.0260)_{17};$$

the angle of this vector with $(0\,\bar{1}\,\bar{2})_{17}$ is 0.9°. If (and perhaps only if) the molecules are colored according to the groups shown in Table 4 the modulation in the $(0\,\bar{1}\,\bar{2})_{17}$ direction is obvious (Fig. 3). The directions of the As—Cl bonds are somewhat different in the two alternating regions and the widths of the two regions (red and blue in Fig. 3) are not the same.

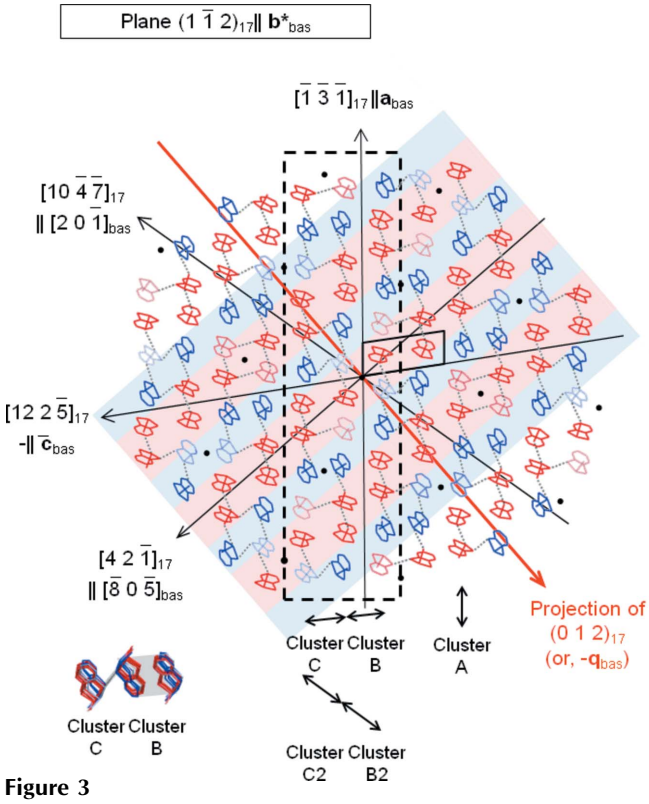

Figure 3
A slice of the structure [approximation (I)] parallel to the plane $(1\,\bar{1}\,2)_{17}$ ‖ $\mathbf{b}^*_{\rm bas}$ (shown in Fig. 2). Molecules are colored according to their (S_2C_6),$(\bar{1}\,\bar{1}\,4)_{17}$ angles (Table 4). Interatomic contacts shorter than $\Sigma_{\rm VDW}$ are marked. The projection of the modulation wave $\mathbf{q}$ is marked in red; it makes an angle of 78° with $(1\,\bar{1}\,2)_{17}$ ‖ $\mathbf{b}_{\rm bas}$. The inversion centers that lie in the plane are marked. The $\mathbf{a}_{\rm bas}$ and $\mathbf{c}_{\rm bas}$ axes are shown as solid black lines.

2.4. Refinement of the average structure

The structure of the average (*i.e.* unmodulated, Z' = 1) cell (Fig. 4) was then determined using the main reflections only. While the results of this refinement are necessarily imprecise they provided important clues when we were trying to understand the modulation. As mentioned above, two orientations of the S_2C_6 dithiolate ligand were found; the more frequent orientation [hereafter, A; occupancy factor 0.592 (2)] corresponds to a (S_2C_6), $(\bar{1}\,\bar{1}\,4)_{17}$ [‖$(0\,1\,2)_{\rm bas}$] angle of 62° (compare dimers A/A′, F/G, H/I, L/M and N/O in Fig. 1 and Table 4) while the other orientation (B) corresponds to an angle of 32° (compare dimers D/E and J/K).

Even with the imposition of restraints some of the displacement ellipsoids for the 12 C atoms of the average cell were non-positive definite. When the C atoms were refined isotropically the displacement ellipsoids for the As, Cl and S atoms were still quite eccentric. The final agreement factors R_1 and wR_2 are 0.103 and 0.264 for 116 variables, 1848 reflections [1465 of which have $I > 2\sigma(I)$], and 110 restraints. The poor agreement is an indication of the significance of the modulation. The ratio of the occupancy factors (0.59:0.41; s.u. 0.005) seems to be consistent with the division by orientation angle of the molecules into groups (Table 4).

2.5. Superspace refinement

The significant deviation of the modulation vector component along $\mathbf{b}^*_{\rm bas}$ [−3.187 (2)/17] from the commensurate value −3/17 means that the structure can never be fully described in a supercell approximation or as a commensurately modulated structure. The deviation from the commensurate value, however, is only about 0.187/17 so that the wavelength

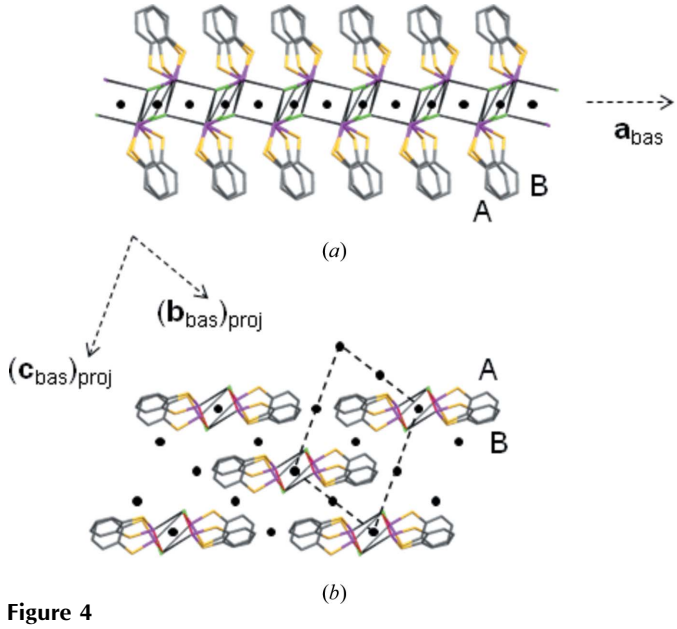

Figure 4
View of the average structure as refined using the main reflections only of the incommensurate integration. The inversion centers are marked as are the two major molecular orientations A and B. (*a*) Ribbon analogous to that shown in Fig. 1. (*b*) View along $\mathbf{a}_{\rm bas}$ of the stacks (compare with Fig. 2).

connected with the incommensurability is about (17/0.187)**b** = 91*b* = 759 Å, which means that the effect has a very smooth character. In the other two crystallographic directions the deviations from commensurability are more than ten times smaller.

As a starting point for the incommensurate refinement we used the average structure described above after adding small, random atomic displacements to break the symmetry. The structure was then refined with the August 2012 version of *JANA*2006 (Petříček *et al.*, 2006), with the final model including harmonic waves up to the fourth order for positional and harmonic ADP modulations. Information about this refinement is given in Table 5. Note that the agreement factors for the conventional and superspace refinements are not quite comparable because of differences in the lists of included reflections. Comparisons are described more fully below.

Two commensurate superstructure approximations were also refined using *JANA*2006. For these the components of the modulation vector were modified to the closed commensurate values. The refinements for $t_0 = 0$ and $t_0 = \frac{1}{2}$ (only these two sections lead to the centrosymmetric space group $P\bar{1}$ for the supercell approximation) give almost the same fit as the incommensurate model. Even though the fits for all the refinements are the same, the two commensurate solutions ($t_0 = 0$ and $t_0 = \frac{1}{2}$) are not equivalent. The incommensurate solution can be used to show that different supercell approximations are possible structure arrangements in the crystal. Note that none of the inversion centers of the commensurate approximation is reproduced exactly in the incommensurate model even though the incommensurate model is centrosymmetric. Small deviations from commensurate values of the components of the modulation vector mean that the local arrangement close to the 'inversion-related dimers' is always slightly noncentrosymmetric.

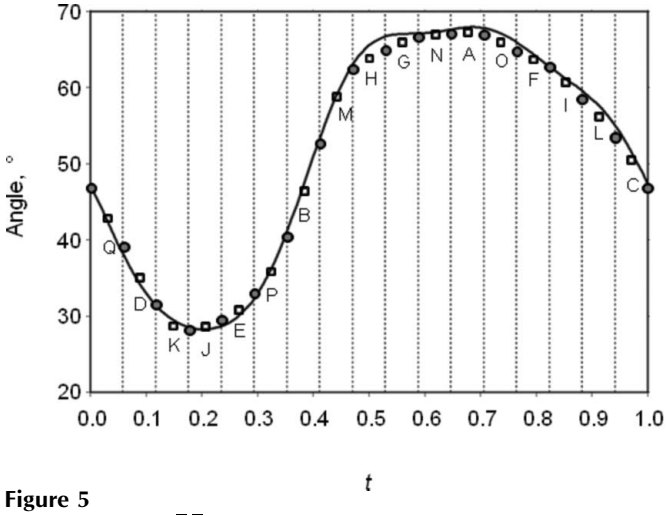

Figure 5
Plot of the (S_2C_6),$(\bar{1}\,\bar{1}\,4)_{17}$ angle as a function of the superspace variable *t*. The vertical lines are drawn at $t = n/17$, $n = 0$–17 as guides to the eye. The angles determined during the conventional refinements are plotted at intervals of 1/17th as well. While agreement between those individual values and the curve is imperfect because the values from the commensurate refinements are only approximations and because the directions of **q** and of the sequence of individual angles points are not quite the same, the superposition shows that the various models are consistent. The points for the $t = \frac{1}{2}$ commensurate approximation (empty squares) are labeled (*cf.* Fig. 1); labels for the $t = 0$ commensurate approximation (filled circles) are available with the supplementary material.

Table 5
Experimental details for the refinement of the incommensurate description.

Fields that are the same as in Table 1 have been omitted.

	Incommensurate model
Crystal data	
Crystal system, space group	Triclinic, $P\bar{1}(\alpha\beta\gamma)$†
Wavevectors	**q** = 0.29482 (12)**a*** − 0.18747 (12)**b*** − 0.4715 (2)**c***
a, *b*, *c* (Å)	4.8103 (2), 8.3518 (3), 11.0375 (5)
α, β, γ (°)	70.123 (2), 81.344 (3), 79.003 (3)
V (Å^3)	407.58 (3)
Z	2
Data collection	
Absorption correction	Multi-scan *SADABS* (Sheldrick, 2008*b*)
T_{min}, T_{max}	0.54, 0.63
No. of measured, independent and observed [$I > 2\sigma(I)$] reflections	32 057, 16 388, 11 119
R_{int}	0.033
$(\sin\theta/\lambda)_{max}$ (Å^{-1})	0.647
Refinement	
$R[F^2 > 2\sigma(F^2)]$, $wR(F^2)$, *S*	0.045, 0.116, 1.34
No. of reflections	16 388
No. of parameters	811
No. of restraints	0
H-atom treatment	H-atom parameters constrained
$\Delta\rho_{max}$, $\Delta\rho_{min}$ (e Å^{-3})	0.91, −0.79

† Symmetry codes: (i) x_1, x_2, x_3, x_4; (ii) $-x_1, -x_2, -x_3, -x_4$. Computer programs: *EVAL*15 (Schreurs *et al.*, 2010), *JANA*2006 (Petříček *et al.*, 2006).

These refinement results do demonstrate that for strictly commensurate structures with pseudoinversion symmetry it is always worthwhile testing different *t*-sections that lead to the same supercell space group in order to avoid false minima and find the best model.

A *t*-plot of the (S_2C_6),$(\bar{1}\,\bar{1}\,4)_{17}$ angle as determined in the superspace refinement is shown in Fig. 5. The plot demonstrates that this interplanar angle is a good measure of the modulation.

2.6. Qualitative difference between superstructure approximations (I) and (II); conventional refinements of approximation (II)

The program *Mercury* (Macrae *et al.*, 2008) was used to compare the approximate supercell structure first solved and refined conventionally [*i.e.* superstructure approximation (I), which was later identified as the $t_0 = \frac{1}{2}$ section] and what will be called superstructure approximation (II), *i.e.* the $Z' = 17$ superstructure approximation corresponding to the $t_0 = 0$ section of the incommensurate refinement.[4] We were not able

[4] It would perhaps be more logical to refer to the $t_0 = 0$ section as approximation (I) and the $t_0 = \frac{1}{2}$ section as approximation (II), but the superstructure approximation corresponding to the $t_0 = \frac{1}{2}$ section was found first and much of the interpretation of the structure was based on it.

to superpose the two models satisfactorily by applying origin shifts of 0 or $\frac{1}{2}$ along the three cell axes.

A satisfactory overlay of superspace approximations (I) and (II) could be made with the program *Mercury* (Fig. 6), but doing so required an origin shift that affects the location of the crystallographic inversion centers. In approximation (I) ($t_0 = \frac{1}{2}$) a crystallographic inversion center lies within a dimer (A$\cdots$A′) in which the $(S_2C_6),(\bar{1}\,\bar{1}\,4)_{17}$ angle (68.0°) is large, but in approximation (II) the crystallographic inversion center lies within a dimer relating molecules for which the $(S_2C_6),(\bar{1}\,\bar{1}\,4)_{17}$ angle is small (28.1° in dimer 5$\cdots$5′). In each case there is an approximate inversion center within the dimer that is strictly centrosymmetric in the other approximation. The difference between the two superstructure approximations does not affect the relationship of adjacent ribbons in any significant way; overlays for three adjacent dimer ribbons look very much like the overlay shown in Fig. 6.

An approximate supercell structure derived from the $t_0 = 0$ approximation (II) was then refined conventionally to convergence in essentially the same way as described above for approximation (I) (Table 1). A comparison of the two refinements shows that the measured diffraction data cannot distinguish between the two models. The fit for approximation (II) is marginally better, but it would be difficult to argue that it is significantly better. The correspondence of the $(S_2C_6),(\bar{1}\,\bar{1}\,4)_{17}$ angles for the best superposition of the two approximations is given in the supplementary material.

2.7. Additional refinements

The *DENZO* (Otwinowski & Minor, 2006; commensurate approximation) and *EVAL*15 (Schreurs *et al.*, 2010) integrated data sets [24 396 and 16 388 unique reflections, with 8774 and 10 864 reflections having $I > 2\sigma(I)$] are not quite comparable. The *EVAL*15 set, which is smaller but less noisy, contains reflections above $\theta = 25°$, but does not contain the satellites with $m = 5 - 8$. The larger *DENZO* set contains the higher-order satellites (most of which are very weak) but no reflections with $\theta > 25°$. In order to better compare the two sets of intensities (1) both approximations were refined conventionally using a set of reflections derived from the *EVAL*15 set by assuming that the modulation vector is commensurate [*i.e.* $m(5/17, -3/17, -8/17)$, where m is the satellite order], and (2) refinements of both approximations with both data sets were made using only the 12 731 unique reflections that occur in both sets. Convergence problems were encountered in all six of these refinements but were more severe in the last four. The final models from the six refinements are very similar to those described in Table 1. More information is provided in the supplementary material.

2.8. CSD searches

The CSD (Version 5.33, November 2011 plus updates through August 2012) was searched for error-free structures having three-coordinate As and Sb atoms bonded to two S atoms and one Cl atom. The number of hits was 26 for As and 7 for Sb, but those numbers were reduced to 8 and 6 after the removal of compounds (*e.g.* sterically constrained cyclic dimers; Cangelosi *et al.*, 2010, and references therein) in which short non-bonded contacts to Cl or S atoms are impossible. Information about the hits is given in the supplementary material.

Searches were also carried out for three-coordinate As and Sb atoms bonded to one S atom and two Cl atoms, but the number of hits was small (four each for As and Sb, some of which are very closely related). They added little information and so were not considered further.

2.9. Energy calculations

Intermolecular energy calculations were carried out at the atom–atom level using the *AA-CLP* force field, recently

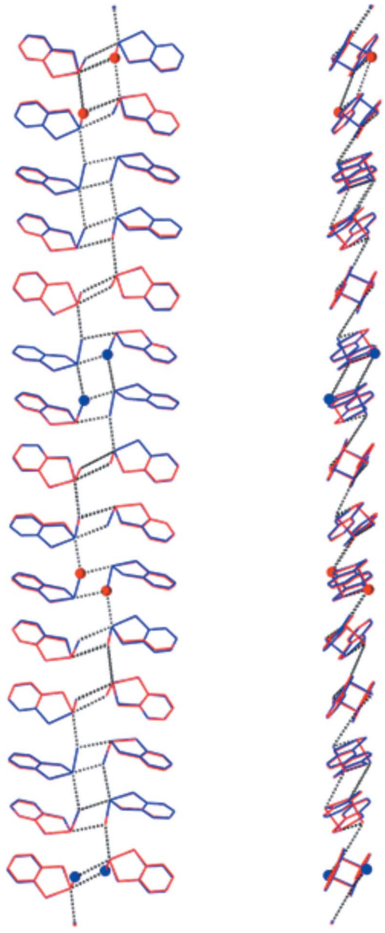

Figure 6
Two views of a superposition of the dimer ribbon for superstructure approximation (I) (red) and (II) (blue); the overlap of the two approximations is so good that it is difficult to distinguish the red and blue drawings. Fifteen dimers of each are shown, with the top nine unique for approximation (I) and the bottom nine unique for (II). The Cl atoms next to the inversion centers within the dimers (lower half of the drawing) and between the dimers (upper half of the drawing) are shown as small spheres. The two models can be superposed very well, but the crystallographic inversion centers are displaced by five dimers between the two models. The $(S_2C_6),(\bar{1}\,\bar{1}\,4)_{17}$ angle for the dimer that lies on an inversion center is quite different for the two models. The crystallographic inversion centers in one superstructure approximation are approximate inversion centers in the other.

developed to reproduce enthalpies of vaporization and sublimation for organic materials (Gavezzotti, 2011). Details are provided in the supplementary material.

3. Results

3.1. Comparison of the conventional and superspace refinements

As judged by the usual agreement factors all refinements [the superspace refinement and the conventional refinements of the superstructure approximations (I) ($t_0 = \frac{1}{2}$) and (II) ($t_0 = 0$)] are of similar quality and lead to the same general description of the atomic positions (Tables 1 and 5). The superspace refinements, however, are preferable because the modulation vector component along $\mathbf{b}^*_{bas}$ is clearly not a simple ratio of integers. The superspace description, however, is more difficult to visualize using standard structure–display programs. The structure will therefore be discussed in the approximate $P\overline{1}$, $Z' = 17$ supercell. Approximation (I) will be discussed except in the case of significant differences between the two models.

3.2. Overview of the structure

In the average structure (*i.e.* the disordered $Z' = 1$ structure determined by ignoring the satellite reflections, Fig. 4); pairs of molecules are arranged around inversion centers to form what appear to be dimers, which are then stacked. The resulting segregation of As—Cl moieties may be taken as an indication that molecules in the crystal are stabilized by some kind of As···Cl interaction. There are also inversion centers between dimers. In the commensurately modulated superstructure approximation (Fig. 1) only one of the nine independent dimers is located on a crystallographic inversion center; the other eight lie on approximate centers. Within the dimers all the As···Cl distances are shorter than the sum of the van der Waals radii (Σ_{VDW} = 1.85 + 1.75 = 3.60 Å; Bondi, 1964), although some are considerably shorter (less than Σ_{VDW} − 0.25 Å) than others (Table 3).

All the individual molecules are very similar; overlays of the 17(16)/2 = 136 pairs of molecules for each of the two approximate commensurate models lead to r.m.s. deviations between the 10 pairs of corresponding atoms in the range 0.01–0.15 Å (average 0.06 Å). When the deviations are at the high end of that range it is usually clear that the C_6S_2As fragments line up well but that the Cl atoms are slightly offset, *i.e.* that the S—As—Cl angles vary a little.

In 11 of the 17 independent molecules of approximation (I) [10 of 17 in (II)] the As atom makes a second short (*i.e.* < Σ_{VDW}) contact to one of the Cl atoms of a neighboring dimer (Fig. 1 and Table 3). The geometry around these As atoms is approximately pyramidal, with the As—Cl covalent bond axial. The intermolecular As···Cl contacts are approximately *trans* to As—S bonds.

These ribbons of dimers extend along $[1\ 3\ 1]_{17}$ (*i.e.* $\parallel -\mathbf{a}_{bas}$), and are arranged so that 10 of the 17 molecules make S···S inter-ribbon contacts (five unique) shorter than Σ_{VDW} = 3.60 Å (Table 3 and Fig. 2); the remaining seven S···S inter-ribbon contacts are only slightly longer.

3.3. Energy calculations

The energy calculations indicate that dispersion energy is, by far, the most important stabilizing factor, a result not unexpected given the chemical nature of the molecules. The main providers of dispersion are the polarizable ring π-system electrons, but the diffuse and polarizable As and Cl 3*s* and 3*p* electrons also contribute (see the supplementary material).

A plot of the energy *versus* centroid–centroid distance for pairs of molecules having interaction energies < −4.0 kJ mol^{-1} is shown in Fig. 7, in which contacts of the same type (17 or 9 unique depending on the location relative to the inversion centers) are enclosed in ellipses. The most consistently favorable interactions (cluster B in Fig. 7; molecules adjacent along $[12\ 2\ \overline{5}]_{17}$) lie within the gray parallelograms marked on Fig. 2. The next most favorable cluster (A) is composed of pairs of molecules adjacent in one half of the dimer ribbon (*i.e.* adjacent along $[1\ 3\ 1]_{17}$). The energies of the contacts in cluster A are more variable than those in B because the dominant dispersion interactions between the rings differ with their orientations, and because the aromatic rings in cluster A adopt a wider range of stacking/offset arrangements than those in cluster B (Fig. 1).

The third most favorable cluster (C; molecules also adjacent along $[12\ 2\ \overline{5}]_{17}$) shows the most variation. This cluster is composed of pairs of molecules that sometimes have short S···S contacts (filled triangles). These S···S contacts are, however, in the middle of the cluster range rather than at the short end. The significance of the S···S contacts is therefore uncertain.

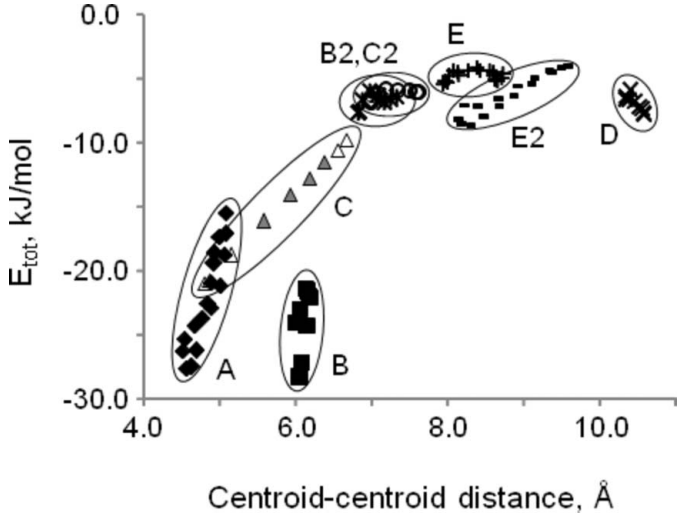

Figure 7
A scatterplot showing the molecule–molecule interaction energies < −4.0 kJ mol^{-1} as a function of the distance between the mass-weighted molecular centroids. Each type of interaction is represented by a different symbol; the symbols of each type are surrounded by an ellipse. The designations of the groups are explained in the text and in the supplementary material. The more compact the groups the less the interactions vary with the structural modulation.

3.4. The modulation wave

Since the structure is so clearly modulated it seemed (at least to those of us who are small-molecule crystallographers) that it should be possible to find a direction in the approximate supercell structure in which adjacent molecules are related by small translational shifts and/or regular orientational changes. The direction found ($[10\,\overline{4}\,\overline{7}]_{17} \parallel [2\,0\,\overline{1}]_{bas}$; Fig. 8) is not especially close to the vector $\mathbf{q}_{bas}$, with which $[10\,\overline{4}\,\overline{7}]_{17}$ makes an angle of 18.0° (Figs. 2 and 3). Along **q**, however, the molecules are not in close contact, which they are along $[10\,\overline{4}\,\overline{7}]_{17}$.

Along $[10\,\overline{4}\,\overline{7}]_{17}$ ($\parallel [2\,0\,\overline{1}]_{bas}$) orientations A and B alternate, except near the crystallographic inversion centers, where the $(S_2C_6),(\overline{1}\,\overline{1}\,4)_{17}$ angle has intermediate values. The details of the modulations in the two superstructure approximations vary slightly (see the supplementary material) but the overall features are the same. Fig. 5 shows that the molecular orientation angles in the sequence shown in Fig. 8 for molecules labeled on the left or labeled on the right (*i.e.* for every second molecule) are very consistent with the *t*-plot of that angle. Along $[10\,\overline{4}\,\overline{7}]_{17} \parallel [2\,0\,\overline{1}]_{bas}$ the orientation angles for every second molecule track the modulation even though **q** makes an angle of *ca* 18° with that direction.

The effects of the modulation are almost certainly most important along the direction $[12\,2\,\overline{5}]_{17} \parallel -\mathbf{c}_{bas}$, which lies within the plane $(1\,\overline{1}\,2)_{17} \parallel \mathbf{b}^*_{bas}$ (Figs. 2 and 3) and includes the interactions of clusters B and C. The modulation along $[12\,2\,\overline{5}]_{17}$ is not, however, as smooth as it is along $[10\,\overline{4}\,\overline{7}]_{17}$, parallel to which the intermolecular interactions are much weaker. The plane $(1\,\overline{1}\,2)_{17}$ is important because the five most important sets of intermolecular interactions all lie within that plane. Molecular layers parallel to that plane are connected by As···Cl interactions (Fig. 2).

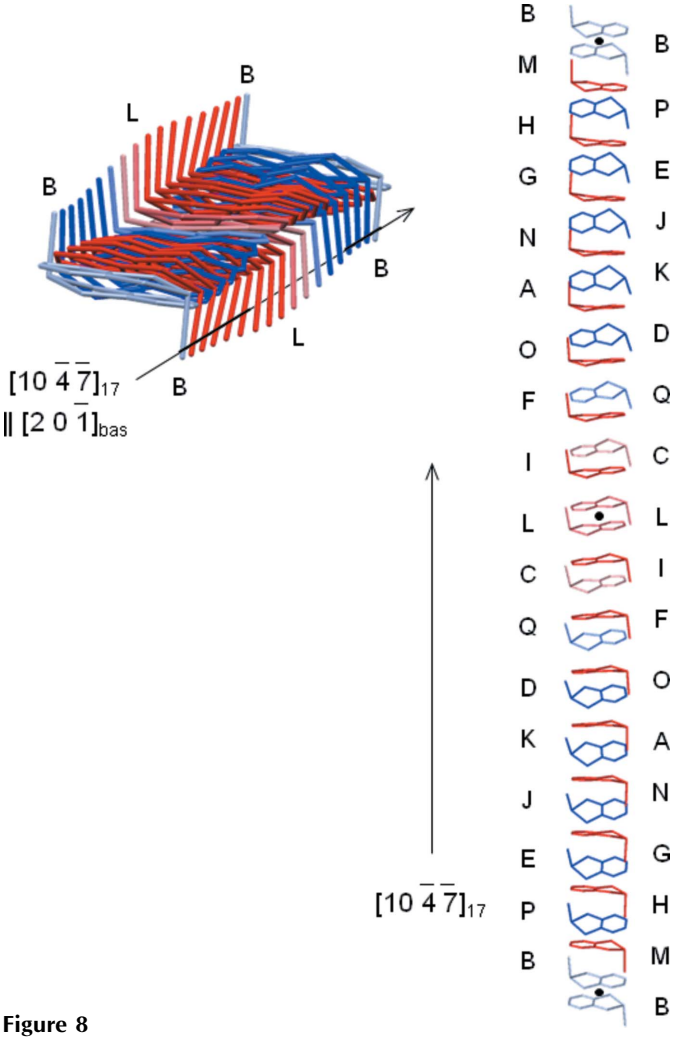

Figure 8
Two views of the modulation as found in superstructure approximation (I). Molecules are colored according to their $(S_2C_6),(\overline{1}\,\overline{1}\,4)_{17}$ angles (Table 4). The direction $[10\,\overline{4}\,\overline{7}]_{17}$ ($\parallel [2\,0\,\overline{1}]_{17}$) makes the pattern of small displacements most obvious even though that direction is not parallel to the modulation (angle is 18.0°). Along $[10\,\overline{4}\,\overline{7}]_{17}$ the molecules are in close contact but along **q** they are not; the sequence along **q** shown in Fig. 5 corresponds to the molecules labeled on the left or to the molecules labeled on the right. One complete period of the modulation is shown. The inversion centers are marked in the view on the right. The modulation in approximation (II) (see text and supplementary material) is very similar.

4. Discussion

4.1. Comparison with the Sb analogue

The molecules in crystals of the Sb-containing analogue (Shaikh *et al.*, 2006; *Pbca*; $Z' = 1$) form layers perpendicular to **c** in which there are two quite short Sb···Cl contacts (3.36 Å) and one somewhat short Sb···S contact (3.67 Å).[5] The geometry around the Sb atom is that of an octahedron composed of three bonded and three non-bonded atoms. While the Sb and Cl atoms lie in the layers; the dithiolate ($C_6H_4S_2$) parts of the molecules are nearly perpendicular to them. The aromatic rings of molecules in adjacent layers interleave to form 'organic' layers that separate layers composed of As and Cl atoms. This structure is impossible for the As compound because As—Cl and As—S bonds are 0.2 Å shorter than Sb—Cl and Sb—S bonds. A change from Sb to As would, because of the glide operations, cause the layer to contract in two directions so that there would not be enough space for interleaving of the C_6 aromatic rings.

4.2. As···Cl and S···S attractions?

The tendency in crystal structures towards spatial segregation of atom types is well known; the tendency of electron-rich atoms to have short contacts has led to the concept of 'secondary bonding interactions' (SBIs; Alcock, 1972) among such atoms.

The subject of closed-shell interactions has been well discussed (Pyykkö, 1997, and references therein). Such interactions are said to be 'ubiquitous' in the chemistry of Pb^{II}, Bi^{III}, Te^{IV} and I^{III} (Starbuck *et al.*, 1999; see also Cozzolino *et al.*, 2011) and are well known for Sn^{II} (Haiduc, 2007). Contacts

[5] The values of the van der Waals radii used are those taken from Bondi (1964) and included in the program *Mercury* (Macrae *et al.*, 2008). Bondi did not give a radius for Sb so a value of 2.00 Å is used in *Mercury*; the values for S and Cl are 1.80 and 1.75 Å. The value given by Mantina *et al.* (2009) is slightly longer at 2.06 Å.

substantially shorter than Σ_{VDW} and in directions approximately parallel to existing covalent bonds can then be expected for Sb^{III} compounds, which is what we found in the CSD search. The case for SBIs involving As atoms (Carter *et al.*, 2007) is less strong, but the CSD search suggests that As···Cl contacts are common.

Short S···S contacts have also been discussed (Row & Parthasarathy, 1981; Bleiholder *et al.*, 2006), particularly as they occur within and between molecular stacks such as those in organic conductors built from tetrathiafulvalene and its derivatives.

In this context the warnings of Dunitz & Gavezzotti (2005, 2009) and Gavezzotti (2010) against overinterpretation of specific atom–atom contacts is pertinent. Still, short, closed-shell contacts between electron-rich atoms are so common that they must be, at least on average, favorable, if only because they allow matching of atomic polarizabilities, which are related to dispersion energies and which are much larger for As, Cl and S than for first-row atoms. The energy calculations made for DTAsCl, however, provided little support for the importance of As···Cl and S···S contacts (see the supplementary material). While the contacts involving the As, Cl, and S atoms may be significant, they seem to be considerably less important than the contacts between the aromatic ring systems.

4.3. Reasons for the modulation

Experience suggests that in a favorable crystal structure of DTAsCl the aromatic rings should form either stacks or a herringbone pattern. In the case of a pattern of stacks, which would probably be the lower-energy arrangement (cluster A in Fig. 7), then the As and Cl atoms might be expected to all lie on one side of a stack because the lengths of As···Cl contacts are compatible with the distances between stacked aromatic rings and because that arrangement would segregate atoms having similar polarizabilities.[6] For similar reasons the As/Cl regions of two stacks would likely be adjacent (hence the dimer ribbons). The angles between the As—Cl or As—S vectors and the As···Cl vectors should be large so as to minimize repulsions. A consideration of polarizabilities also suggests that short S···S contacts can be anticipated. Finally, space should be filled densely, and the value of Z' should be low because low values of Z' are so overwhelmingly frequent in the CSD that they must be favorable. Examination of the DTAsCl structure (Fig. 2) shows that all of these expectations are fulfilled except for that of a small asymmetric unit.

It seems very likely that the origin of the modulation lies within the packing of adjacent ribbons. An isolated dimer-ribbon fragment (such as might exist in a concentrated solution) would almost certainly be nearly periodic. Since the dithiolate units in orientation A [angle $(S_2C_6),(\bar{1}\,\bar{1}\,4)_{17}$ *ca* 60–65°] can fill space densely with As···Cl distances more than 0.1 Å shorter than Σ_{VDW} (*e.g.* dimers F/G and H/I in Fig. 1) there would be no reason for a complicated alternation pattern. Orientation B with its smaller $(S_2C_6),(\bar{1}\,\bar{1}\,4)_{17}$ angles (dimers D/E and J/K in Fig. 1) lowers the packing density and makes the stacking less favorable, and so would be unlikely to occur in isolated ribbon fragments.

Fig. 2 shows that the ribbons are packed in the way expected for columnar objects that have a parallelepipedal cross section. Each ribbon has six near neighbors.

The refinement in the disordered $Z' = 1$ average cell shows that in a simple structure in which all molecules had orientation A there would be impossibly short (some less than $\Sigma_{VDW} - 0.4$ Å) S···C, S···H and C···C intermolecular contacts in the gray shaded areas (Figs. 2 and 3). Sets of interfering molecules extend along $\mathbf{c}_{bas}$ ($\|[12\,2\,\bar{5}]_{17}$; cluster B) and also along $[2\,0\,\bar{1}]_{bas}$ ($\|[10\,\bar{4}\,\bar{7}]_{17}$; cluster B2).

Those impossibly short contacts are relieved in the modulated structure by the presence of molecular orientation B. The B orientation, however, causes problems along the ribbon axis ($\mathbf{a}_{bas} \| [\bar{1}\,\bar{3}\,\bar{1}]_{17}$). If two B molecules were adjacent in a ribbon they would be impossibly close (C···C < $\Sigma_{VDW} - 0.5$) unless the ribbon were stretched substantially. The presence of a B molecule in the ribbon also causes problems if it is next to an A molecule; in an unmodulated structure there would be intra-ribbon S···C contacts 0.34 and 0.40 Å shorter than Σ_{VDW}. These latter problems, however, can be turned into packing advantages by adjustments to the spacings as well as the orientations of the molecules. Hence the irregularities obvious in Fig. 1.

We conclude that the structure is modulated in order to find a balance between favorable contacts within and between ribbons. The ribbons exist because they allow stacking interactions and As···Cl contacts. The observed arrangement of the ribbon columns is the only one that allows space to be filled densely, but it leads to very unfavorable inter-ribbon interactions that cannot be resolved easily. A second molecular orientation (B) occurs to relieve inter-ribbon contacts, but the B orientation must be accompanied by shifts along the ribbon axis to ease the resulting too-short contacts within the ribbons. The best compromise requires a distortion wave that is incommensurate (or that is very long in a commensurate approximation). It is impressive, however, that a single (and centrosymmetric) modulation can solve so many different packing problems well enough to allow growth of good-sized, ordered crystals that show no signs of disorder or twinning.

4.4. A few more comments about the modulation

All the dimers in the ribbon (Fig. 1) have approximate local inversion symmetry. The average difference of the $(S_2C_6),(\bar{1}\,\bar{1}\,4)_{17}$ angles between the molecules within a dimer is 2.8° in model (I) and 2.7° in model (II) (Fig. 6). In model (I) the largest difference (7.2°) is between the two molecules of dimer (P/Q) that lies next to an inversion center; in model (II) the largest differences are within dimers 9/1 and 8/2 (6° each).

Within a ribbon the As···Cl contacts that are longer than Σ_{VDW} are mostly associated with molecules that have the B orientation. Space-filling models calculated with *Mercury* (see the supplementary material) show that there are gaps on both

[6] If the As/Cl regions alternated from one side of the stack to the other then they would be separated by C/H regions.

sides of the C_6 rings of the B molecules while the rings of the A molecules are in much better contact.

In the average $Z' = 1$ refinement the ends of the molecules are not in especially close contact (cluster D in Fig. 7). The shortest H···H contacts along the horizontal direction of Fig. 2 have lengths 2.29 and 2.24 Å. These contacts are either a little short (Σ_{VDW} = 2.40 Å; Bondi, 1964) or are not (Σ_{VDW} = 2.20 Å; Rowland & Taylor, 1996; Mantina *et al.*, 2009); but in any event the intermolecular interactions in other directions are almost certainly much more important in determining the structure. The spacings for clusters A, B and C, together with the inversion symmetry, determine the cell dimensions.

The energy calculations show that the average energy per molecule is correlated with its orientation angle $(S_2C_6),(\overline{1}\,\overline{1}\,4)_{17}$; on average the B molecules (smaller angles) have total energies *ca* 5 kJ mol^{-1} higher than the more frequent A molecules. The spread of total packing energies E^i over the 17 molecules in the modulated structure is, however, only 6 kJ mol^{-1}, *i.e.* less than 10% (see the supplementary material) of the total lattice energy.

4.5. Why a simpler structure is impossible

No simple structure is possible for DTAsCl because the three directions along which at least some alternation of molecular orientations A and B is required all lie within a plane [*i.e.* within $\mathbf{b}^*_{bas} \parallel (1\,\overline{1}\,2)_{17}$] (Fig. 3). Two of the three directions correspond to clusters A ($\mathbf{a}_{bas}$) and B/C ($\mathbf{c}_{bas}$); the third important direction ($[2\,0\,\overline{1}]_{bas}$; clusters B2 and C2) is that along which the modulation is most obvious (Fig. 8). Because these directions are linearly dependent it is not possible to have a simple alternation pattern along all three.

Examination of the ribbons that extend along $\mathbf{a}_{bas}$ ($\parallel [\overline{1}\,\overline{3}\,\overline{1}]_{17}$) suggests that the motif A···A···B of molecular orientations is common. A 2:1 alternation pattern, however, would lead to the same packing problems as a 1:1 pattern, as would any other 'simple' pattern.

4.6. Why the superspace refinement was important

The conventional indexing, solution and refinement of this structure were so satisfactory that we at the University of Kentucky initially dismissed the idea that the structure might be incommensurate even though we recognized Z' as being both exceptionally large and prime. Furthermore, the *SHELXS* solution (which placed all molecules within a roughly equidimensional asymmetric unit) did not make the modulation obvious. We later learned that while the deviations of diffraction maxima from the positions they would have in a commensurate structure may be very small, an analysis of the positions of tens of thousands of such maxima can reveal a small deviation from commensurability.

Even before considering incommensurability, however, the very high Z' value caused us to look at the structure carefully with the powerful display program *Mercury* (Macrae *et al.*, 2008). After finding the short As···Cl contacts and the dimer ribbons that extend along $[1\,3\,1]_{17}$ we knew that the structure was modulated and knew the orientation of one of the axes of a basic cell. We were not, however, able to find the complete basic cell and the modulation vector until after the first integration using *EvalCCD* (Duisenberg *et al.*, 2003).

We had, perhaps naively, expected to be able to interpret the structure in terms of problem intermolecular contacts in the **q** direction. The molecules, however, are not even in close contact along that direction; rather, the modulation **q** results in alternation patterns along the three direct-space directions in which the intermolecular contacts are most important. Because we kept trying to look along **q** it took some time to find the rather striking modulation along $[10\,\overline{4}\,\overline{7}]_{17}$. We continued searching, however, because the superspace refinement had convinced us there must be a direction in which the modulation would be obvious.

Only the refinement and careful examination of the average ($Z' = 1$) structure allowed us to identify the impossibly short contacts that had to be resolved in a modulated structure; without the results of this refinement we would probably never have found the three coplanar directions in which modulation of the molecular orientations is required. It is perhaps no surprise that a modulation that alleviates packing problems in more than one direction might be incommensurate. The details of the incommensurability are, however, much more difficult to understand, especially along $\mathbf{b}^*_{bas}$.

4.7. Why is this kind of modulation not seen more often?

The number of published incommensurate structures of molecular crystals is small – almost certainly fewer than 100. A search of the CSD for entries including the word 'incommensurate' turned up 35 unique compounds (15 of them organic); searches of other sources [including Schönleber's (2011) review and the Bilbao Crystallographic Server (Aroyo *et al.*, 2006)] found some additional structures (see the supplementary material). There are also a large number of incommensurate inclusion complexes of urea.

Only nine of the molecular incommensurate structures we found are built from a single molecule; the great majority of the incommensurate structures have two sublattices with different spacings. Classic examples of incommensurate structures composed of a single molecule are biphenyl (Baudour & Sanquer, 1983), bis(*N*-methylsalicylideneaminato)nickel(II) and -copper(II) (Steurer & Adlhart, 1983*a*,*b*), thiourea (Zuñiga *et al.*, 1989), and 4,4′-dichlorobiphenyl sulfone (Zúñiga *et al.*, 1993). More recent examples include 2-phenylbenzimidazole (Zúñiga *et al.*, 2006), two larger organic molecules ($C_{22}H_{20}O_3$; Guiblin *et al.*, 2006; $C_{19}H_{27}NO_3Si$; Wagner & Schönleber, 2009), and deuterated thiophene (Damay *et al.*, 2008).

Perhaps the number of such structures is so low because they are truly rare. It may also be, however, that incommensurate molecular structures occur more often but that the modulations are usually either missed or ignored, so that the

structures are described in approximate commensurate supercells.[7] Diffractometers equipped with highly sensitive area detectors, as well as software that makes use of the increased information, are much more likely to find the modulated version of a disordered average structure than were diffractometers equipped with serial detectors. Brighter X-ray beams also raise the probability of observing extra diffraction maxima. Even so, it is easy to overlook modulations in molecular materials because the satellite peaks are usually systematically weak at best. Crystals of DTAsCl have strong satellite peaks because the amplitude of the modulation is large, and because the number of atoms per molecule is low and the average number of electrons per atom high. It is also important that there are strong intermolecular interactions in several directions so that the modulation is more likely to be coherent through large regions of a crystal.

The amount of time necessary to refine and interpret a modulated structure is great enough that it may often seem wiser just to publish a disordered structure in the basic cell. After working on this structure we are sympathetic with that view, but believe that if a modulation is observed it should at least be mentioned.

We have now seen two crystals (this work; Koutentis *et al.*, 2001) in which the presence of strong one-dimensional interactions (*i.e.* packing dominated by ribbons or stacks) led to a modulated structure because of problems with inter-ribbon or inter-stack interactions. We suspect that the presence of ribbons and stacks increases the chances of a modulation, especially if there are no adjustable interactions (like hydrogen bonds) that link those units.

5. Summary

The incommensurate structure of $C_6H_4S_2AsCl$ can be refined nearly equally successfully (as measured by standard criteria) in superspace or as two commensurate superstructure approximations that differ in the location of their crystallographic inversion centers. Integration of the data frames, however, confirmed that the structure is better described as incommensurate even though the deviations from commensurability are small. This result demonstrates that a conventional refinement that is satisfactory by normal standards does not guarantee that the structure is commensurate.

The modulation is best described in terms of the angle made by the C_6S_2 plane with the crystallographic direction $(\overline{1}\,\overline{1}\,4)_{17} \parallel (0\,1\,2)_{bas}$. A smooth variation of this angle along **q** (Fig. 5) leads to alternation patterns in several other directions along which the molecules are in close contact ($[\overline{1}\,\overline{3}\,\overline{1}]_{17}$, $[12\,2\,\overline{5}]_{17}$ and $[10\,\overline{4}\,\overline{7}]_{17}$), or $\mathbf{a}_{bas}$, $\mathbf{c}_{bas}$ and $[2\,0\,\overline{1}]_{bas}$; Figs. 1, 2, 3 and 8). The importance of angular alternation in these directions was discovered by looking at the impossibly close contacts that would result if the structure were disordered in the average, $Z' = 1$ cell. It is impressive that one modulation alleviates several packing problems well enough to permit the growth of crystals that diffract well and that show no signs of disorder or twinning.

The direction in which a small-amplitude modulation is most obvious ($[10\,\overline{4}\,\overline{7}]_{17} \parallel [2\,0\,\overline{1}]_{bas}$; Fig. 8) was only found after considerable searching. Looking in the direction of the **q** vector proved unproductive because along **q** the molecules are not in close contact. If we had not known that there must be a direction in which the modulation is smooth and has a long wavelength we probably would never have found the view shown in Fig. 8.

Because of the greater number of degrees of freedom allowed we found that the conventional refinement revealed aspects of the modulation (*e.g.* the variation of the S—As—Cl angles) that probably would have been missed if only a superspace refinement had been performed. If the modulation is strong enough that there are sufficient data for a conventional refinement then the two types of refinement may provide complementary information.

If the goal is to understand a complicated structure then there is no substitute for time spent looking at it carefully with a powerful display program.

We are very grateful to Dr R. Hooft of Bruker AXS Delft and Dr A. M. M. Schreurs of the University of Utrecht for reprocessing the original frames to give intensity data corresponding to an incommensurately modulated unit cell. We thank Dr M. A. Siegler, now at Johns Hopkins University, for investigating the diffraction pattern at room temperature and after cooling a crystal slowly. We thank Professor A. Gavezzotti for his generous assistance with the energy calculations and their interpretation. It is a pleasure to acknowledge the programmers at the Cambridge Crystallographic Data Centre, without whose powerful visualization program *Mercury* we would not have been able to understand the modulation.

References

Alcock, N. W. (1972). *Adv. Inorg. Chem. Radiochem.* **15**, 1–58.
Allen, F. H. (2002). *Acta Cryst.* B**58**, 380–388.
Aroyo, M. I., Perez-Mato, J. M., Capillas, C., Kroumova, E., Ivantchev, S., Madariaga, G., Kirov, A. & Wondratschek, H. (2006). *Z. Kristallogr.* **221**, 15–27.
Baudour, J. L. & Sanquer, M. (1983). *Acta Cryst.* B**39**, 75–84.
Becker, G., Mundt, O. & Standelmann, H. (1990). *Z. Anorg. Allg. Chem.* **580**, 139–150.
Bleiholder, C., Werz, D. B., Köppel, H. & Gleiter, R. (2006). *J. Am. Chem. Soc.* **128**, 2666–2674.
Bondi, A. (1964). *J. Phys. Chem.* **68**, 441–451.
Cangelosi, V. M., Pitt, M. A., Vickaryous, W. J., Allen, C. A., Zakharov, L. N. & Johnson, D. W. (2010). *Cryst. Growth Des.* **10**, 3531–3536.
Carter, T. G., Vickaryous, W. J., Cangelosi, V. M. & Johnson, D. W. (2007). *Comments Inorg. Chem.* **28**, 97–122.
Cozzolino, A. F., Elder, P. J. & Vargas-Baca, I. (2011). *Coord. Chem. Rev.* **255**, 1426–1438.
Damay, F., Rodríguez-Carvajal, J., André, D., Dunstetter, F. & Szwarc, H. (2008). *Acta Cryst.* B**64**, 589–595.
Duisenberg, A. J. M., Kroon-Batenburg, L. M. J. & Schreurs, A. M. M. (2003). *J. Appl. Cryst.* **36**, 220–229.

[7] In Koutentis *et al.* (2001) one of us described the structure of the perchlorophenalenyl radical ($C_{13}Cl_9$) in the space group *P*3*c*1 with nine independent molecules, each having imposed threefold symmetry, but there was enough disorder in the structure that it now seems likely that the modulation was actually incommensurate.

Dunitz, J. D. & Gavezzotti, A. (2005). *Angew. Chem. Int. Ed.* **44**, 1766–1787.
Dunitz, J. D. & Gavezzotti, A. (2009). *Chem. Soc. Rev*. **38**, 2622–2633.
Gavezzotti, A. (2010). *Acta Cryst.* B**66**, 396–406.
Gavezzotti, A. (2011). *New J. Chem.* **35**, 1360.
Guiblin, N., Fuhrer, C. A., Häner, R., Stoeckli-Evans, H., Schenk, K. & Chapuis, G. (2006). *Acta Cryst.* B**62**, 506–512.
Haiduc, I. (2007). *Appl. Organomet. Chem.* **21**, 476–482.
Kisenyi, J. M., Willey, G. R., Drew, M. G. B. & Wandiga, S. O. (1985). *J. Chem. Soc. Dalton Trans.* pp. 69–74.
Koutentis, P. A., Haddon, R. C., Oakley, R. T., Cordes, A. W. & Brock, C. P. (2001). *Acta Cryst.* B**57**, 680–691.
Macrae, C. F., Bruno, I. J., Chisholm, J. A., Edgington, P. R., McCabe, P., Pidcock, E., Rodriguez-Monge, L., Taylor, R., van de Streek, J. & Wood, P. A. (2008). *J. Appl. Cryst.* **41**, 466–470.
Mantina, M., Chamberlin, A. C., Valero, R., Cramer, C. J. & Truhlar, D. G. (2009). *J. Phys. Chem.* **113**, 5806–5812.
Nonius (1997). *COLLECT* and *DENZO-SMN*. Nonius BV, Delft, The Netherlands.
Otwinowski, Z. & Minor, W. (2006). *International Tables for Crystallography*, Vol. F, 1st online ed., ch. 11.4, pp. 226–235. Chester: International Union of Crystallography.
Petříček, V., Dusek, M. & Palatinus, L. (2006). *JANA*2006. Institute of Physics, Praha, Czech Republic.
Pyykkö, P. (1997). *Chem. Rev*. **97**, 597–636.
Row, T. N. G. & Parthasarathy, R. (1981). *J. Am. Chem. Soc.* **103**, 477–479.
Rowland, R. S. & Taylor, R. (1996). *J. Phys. Chem.* **100**, 7384–7391.
Schönleber, A. (2011). *Z. Kristallogr.* **226**, 499–517.
Schönleber, A. & Chapuis, G. (2004). *Acta Cryst.* B**60**, 108–120.
Schreurs, A. M. M., Xian, X. & Kroon-Batenburg, L. M. J. (2010). *J. Appl. Cryst.* **43**, 70–82.
Shaikh, T. A., Bakus, R. C., Parkin, S. & Atwood, D. A. (2006). *J. Organomet. Chem.* **691**, 1825–1833.
Shaikh, T. A., Parkin, S. & Atwood, D. A. (2006). *J. Organomet. Chem.* **691**, 4167–4171.
Sheldrick, G. M. (2008*a*). *Acta Cryst.* A**64**, 112–122.
Sheldrick, G. M. (2008*b*). *SADABS*. University of Göttingen, Germany.
Starbuck, J., Norman, N. C. & Orpen, A. G. (1999). *New J. Chem.* **23**, 969–972.
Steurer, W. & Adlhart, W. (1983*a*). *Acta Cryst.* B**39**, 349–355.
Steurer, W. & Adlhart, W. (1983*b*). *Acta Cryst.* B**39**, 721–724.
Wagner, T. & Schönleber, A. (2009). *Acta Cryst.* B**65**, 249–268.
Zuñiga, F. J., Madariaga, G., Paciorek, W. A., Pérez-Mato, J. M., Ezpeleta, J. M. & Etxebarria, I. (1989). *Acta Cryst.* B**45**, 566–576.
Zúñiga, F. J., Palatinus, L., Cabildo, P. & Claramunt, R. M. (2006). *Z. Krisallogr.* **221**, 281–287.
Zúñiga, F. J., Pérez-Mato, J. M. & Breczewski, T. (1993). *Acta Cryst.* B**49**, 1060–1068.